ACS APPLIED MATERIALS & INTERFACES

Research Article

www.acsami.org

Indium Tin Oxide-Free Transparent Conductive Electrode for GaN-Based Ultraviolet Light-Emitting Diodes

Ja-Yeon Kim,[†] Jong-Hyun Jeon,[†,‡] and Min-Ki Kwon*[,‡]

[†]Korea Photonics Technology Institute (KOPTI), 9 Chemdan venture-ro, Buk-gu, Gwangju 500-460, Korea

[‡]Department of Photonic Engineering, Chosun University, 309 Pilmun-daero, Dong-gu, Gwangju 501-759, Korea

ABSTRACT: Transparent conducting electrodes are important components of highly efficient ultraviolet light-emitting diodes (UV LEDs). Indium tin oxide (ITO) is commonly used to form a current spreading layer, but its UV-range optical transparency is limited with a low sheet resistance. We demonstrate a simple solution-based coating technique to obtain large-area, highly uniform, and conductive silver-nanowire-based electrodes that exhibit UV-range optical transparency better than that of ITO for the same sheet resistance. The UV LEDs fabricated using this current spreading layer showed improved optical power emission as well as improvement in electrical properties.

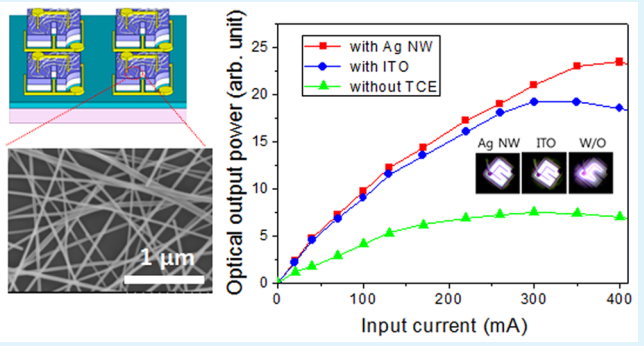

KEYWORDS: *transparent conductive electrode, nanowires, sheet resistance, GaN, light-emitting diodes*

INTRODUCTION

GaN-based ultraviolet light-emitting diodes (UV LEDs) have attracted much attention for applications in fluorescence-based chemical sensing, sterilization, water/air purification, flame detection, and high-density optical data storage.[1,2] In addition, UV LEDs can be used as the source of high-color rendering index white light, and they are therefore one of the most promising candidates for solid-state lighting. However, the luminous efficiency of InGaN based or AlGaN based UV LEDs is still not sufficient for practical application. It is reported that the efficiency of InGaN-based UV LEDs is lower than that of blue LEDs because of the lack of indium-rich regions that act as localized recombination sites, because the indium content in the InGaN active layer is much lower in UV LEDs.[3] In addition, although AlGaN based UV LEDs with emission wavelength shorter than 360 nm have been reported by several groups, the LED quantum efficiency drops dramatically with increasing Al content in order to decrease the wavelength, because of the difficulty in achieving high crystalline quality and doping efficiency in AlGaN at high Al content, suppressing electron overflow from the QW and low extraction efficiency. So, the efficiency of AlGaN-based UV LED is much lower than that of the InGaN blue LED. To improve the efficiency with reducing defect, InGaN-based or AlGaN-based LED have been grown on bulk GaN or AlN substrate. However, the high cost of these methods limits their commercial use. Therefore, one of the problems associated with conventional UV LEDs is the use of nonconductive sapphire as the substrate because it causes the current crowding effect near the p-contact by lateral carrier injection. To solve these problems, researchers have widely used indium tin oxide (ITO) as a transparent conductive electrode (TCE) in InGaN-based LEDs with the advantages of high electrical conductivity and high optical transparency; however, ITO is costly and shows low transparency in the UV range and instability in the presence of acids or bases.[4,5] Therefore, there is a significant need for a novel electrode material that can replace ITO. Promising candidates for ITO replacement in UV LEDs include metal nanowires, single-walled carbon nanotubes (CNTs), and graphene.[6−19] Among these candidates, the silver nanowire (Ag NW) is especially promising because its conductivity ($\sigma_{Ag} = 6.3 \times 10^7$ S m^{-1}) is higher than that of carbon-based CNTs and graphenes. In addition, low contact resistance on the order of 1×10^{-5} Ω cm^2 has been obtained from Ag-based Ohmic contacts annealed in ambient oxygen.[20−22] Graphene was reported to have a sheet resistance of >1000 Ω/sq for single layers, 800−900 Ω/sq for bilayers, and 450−600 Ω/sq for trilayers with a transmittance of 95−80% and CNT was reported to have a sheet resistance of 200 Ω/sq at an average transmittance of 80%.[6−13] This comparison shows that the sheet resistance of TCEs made of CNT or graphene with optical transmittance above 85%, is at least 1 order of magnitude higher than that obtained by using an ITO-based TCE, resulting in a decrease in the current injection efficiency and current crowding. However, it is reported that the Ag NW-based TCE resulted in an electrical and optical performance comparable to that of the ITO-based TCE, a result that is relevant to overcome the above-mentioned limitations of ITO: For example, a large-area Ag NW-based TCE with a sheet resistance of ∼50 Ω/sq at a transmittance of ∼90% was realized by Scardaci et al. and Wu et al.[9,10] In

Received: December 26, 2014
Accepted: April 1, 2015
Published: April 1, 2015

DOI: 10.1021/am509116s
ACS Appl. Mater. Interfaces 2015, 7, 7945−7950

addition, Ag NW-based TCEs shows higher transparency in UV range than ITO. Ag NW-based TCEs could also be created from simple methods such as drop casting, spray coating, and spin coating, processing costs that are significantly lower than those of ITO-deposition methods can be realized. Despite the many advantages of Ag NWs as ITO replacement for fabricating TCEs, there are few reports on the characteristics of LEDs with a Ag NW-based TCE. Seo et al. reported the hybrid AgNW/graphene TCE for UV LED.[18,19]

In this study, we demonstrate an UV LED with a single Ag NW-based TCE deposited by the simple solution based coating method. After optimization of deposition condition, the Ag NW-based TCE showed a sheet resistance of 30−40 Ω/sq and an optical transmittance of over 85% at UV wavelength, which are better than the characteristics of ITO. The electrical and optical properties of a UV LED with a Ag NW-based TCE were better than those of a UV LED with an ITO-based TCE.

EXPERIMENTAL SECTION

Fabrication of UV LED with Ag NW TCE. Ag NWs were synthesized according to a reported procedure[18] and dispersed in DI water (0.5 wt %). The GaN-based UV LED structure (operating at a dominant emission peak of 385 nm) was grown on c-plane (0001) sapphire substrates using metal−organic chemical vapor deposition. The LEDs consisted of the following layers: a 4 μm thick Si-doped n-GaN layer, multiple-quantum-well (MQW) active layer consisting of five periods of undoped InGaN wells and undoped GaN barriers, and a 0.15 μm thick Mg-doped p-GaN layer with a hole concentration of 3×10^{17} cm^{-3}. Figure 1 shows a schematic of the fabrication process for the UV LED with the Ag NW-based TCE: (a) Ag NWs were deposited by spin coating over p-GaN to obtain a TCE. For a comparative study, a 200 nm thick ITO layer was deposited to form a TCE. (b) The spin-coated Ag NW layer was annealed at 150 °C for 10 min to form a Ohmic contact. (c) The region to be patterned was covered with a protective photoresist (PR) as an etch mask. (d) To fabricate the LEDs, which were 500 × 500 μm in size, Ag NW and ITO layers were etched using a dilute $HNO3/H_2O$ (10:1) and HCl/H_2O (10:1) mixture, respectively. The p-GaN and MQW active layer was subsequently etched using an inductively coupled plasma from Cl_2/BCl_3 source gases until the n-GaN layer was exposed for n-type contact. (e) The PR was then removed using hot acetone. (f) Cr/Au, as n- and p-pad electrode, was deposited by e-beam evaporation.

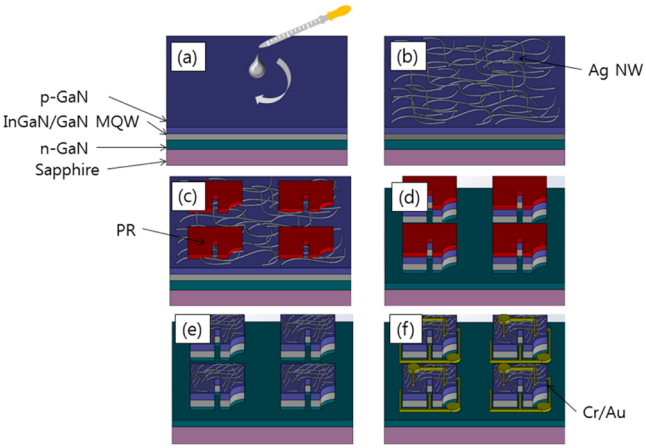

Figure 1. Schematic of the fabrication process for the LED with the Ag nanowire-based transparent conductive electrode.

Instruments and Measurements. Field-emission scanning electron microscopy (FE-SEM) and high-resolution transmission electron microscopy (HR-TEM, JEOL-2100F operated at 200 kV, KBSI Gwangju Center) were used to examine the geometry and morphology of the Ag NWs deposited on the p-GaN surface. The circular pad was patterned on the 1.5-μm-thick *p*-GaN layer using a the standard photolithography technique for measurement of specific contact resistances using a circular-transmission line model (CTLM). The inner dot radius was 100 μm, and the spacing between the inner and the outer radii were 10, 20, 30, 40, and 50 μm. X-ray photoemission spectroscopy (XPS, ESCALAB 250, KBSI Busan Center) was carried out using Al Ka X-ray source in an ultrahigh vacuum system with chamber-based pressure of $\sim 1 \times 10^{-10}$ Torr.

Optical and electrical performances of the spin-coated Ag NWs under various deposition conditions were measured using a UV−vis spectrometer (8453, Agilent) and a four-point probe, respectively.

RESULTS AND DISCUSSION

To form the conductive Ag NW-based TCE, which was comparable to ITO, individual Ag NWs with average 35 nm in diameter and 25 μm in length were used, as shown by TEM images in Figure 2a, b. The figure also shows the network of one or two randomly oriented Ag NWs. The TEM image in Figure 2b shows several nanowires with uniform diameter along their lengths. Optical transmittance over the UV range is an important parameter for TCE application in UV LED. The transmittance was measured using a double polished sapphire as the reference. Figure 2c shows the transmittance of the Ag NW-based TCE with various sheet resistances and the ITO-based TCE on a glass substrate. The transmittance of the ITO-based TCE is dramatically decreased with decreasing wavelength, especially in the UV range. This result shows that ITO is not a suitable material for fabricating the TCE of UV LEDs as shown in Figure 1c. The transmittance of the ITO-based TCE at a wavelength of 385 nm was 81% when the sheet resistance was 33 Ω/sq, whereas that of the Ag NW-based TCEs was 94.3, 92.2, 87.3, and 71.8% when the sheet resistance was 103, 57, 32, and 10 Ω/sq, respectively, as shown in Figure 2c. The transmittance of the ITO-based TCE is slightly lower than that of the Ag NW-based TCE of similar sheet resistance. In addition, as expected, the transmittance was higher when a small volume of Ag NW solution was spin-coated, but this also resulted in higher sheet resistance because a smaller number of NWs connected to form the network.

Figure 2d shows that transmittance of the Ag NW-based TCE decreased dramatically with decreasing sheet resistance because the number of NWs forming the network increased. Figure 2c also shows that optical transmittance of the films was essentially constant across all measured wavelength regions because the optical transmittance of the metal NW film is only dependent on the density of the metal NW network. However, a decrease in the transmittance around short wavelengths of 350 nm can be attributed to the localized surface plasmon resonance.[23] These plasmonic effects can be helpful to improve the light extraction efficiency and tailor the propagation direction.[24,25] In addition, the wavelength-dependent transmittances of Ag NW with different resistances show peak transmittance in wavelength range of 300 nm to 350 nm. This peak transmittance in wavelength range of 300−350 nm can be attributed to the constructive interference with respect to the surface area uncovered by the Ag NW networks.[26] To study the stability of Ag-based TCE, we exposed Ag NW TCE in vacuum and air ambient for 350 h at a room temperature. Figure 2e shows that the sheet resistance was almost the same after 350 h. This result indicates that Ag-based TCE is stable without oxidation.

The dependence of the number of Ag NWs on the sheet resistance can be more clearly seen in the SEM image shown in

DOI: 10.1021/am509116s
ACS Appl. Mater. Interfaces 2015, 7, 7945−7950

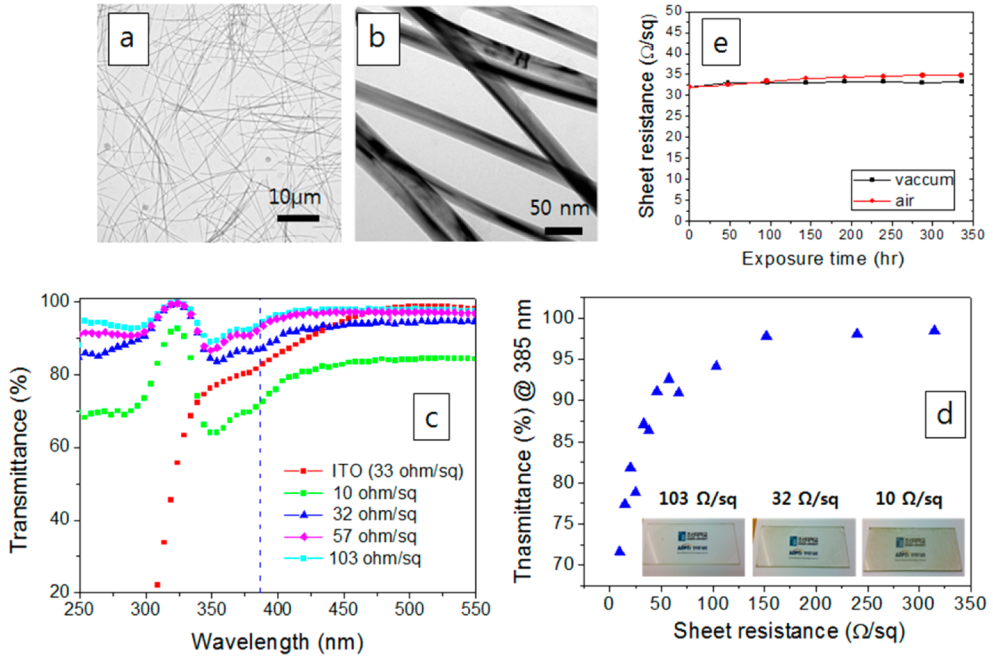

Figure 2. (a) Transmittance electron microscope image, (b) magnified transmittance electron microscope image, (c) transmittance of the Ag nanowire (NW)-based transparent conductive electrode (TCE) with various sheet resistance values, (d) transmittance of the Ag NW-based TCE as a function of the sheet resistance, and (e) sheet resistance of Ag NW-based TCE as a function of exposure time in vacuum and air.

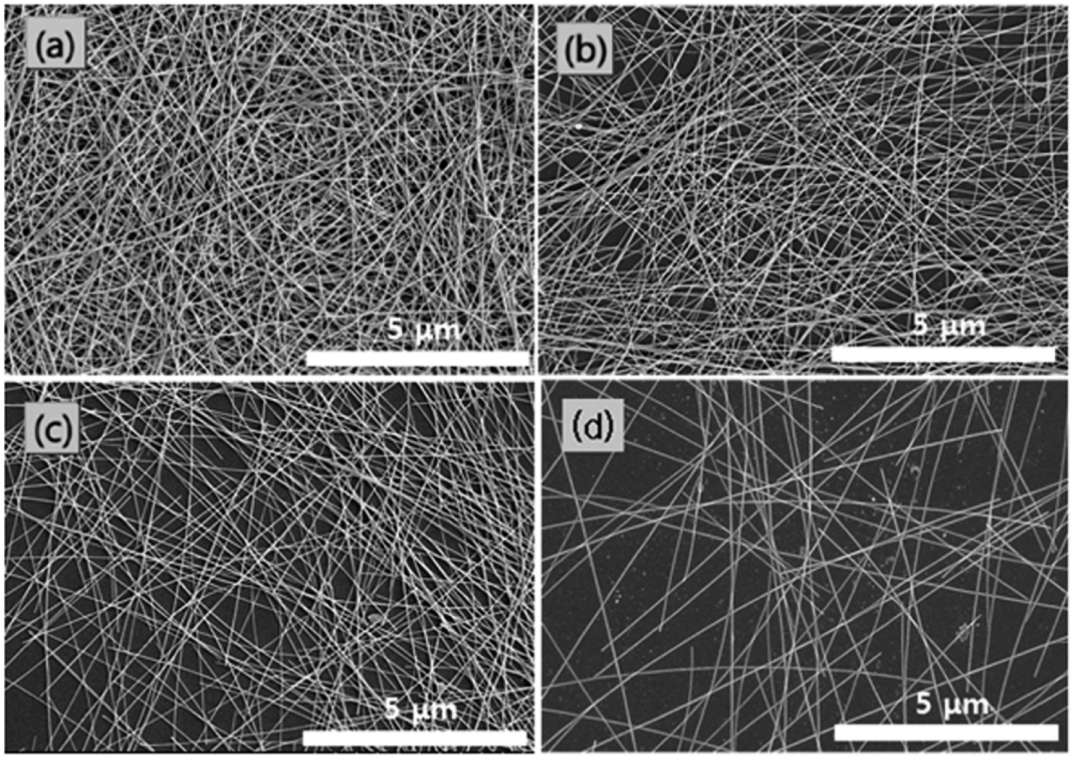

Figure 3. SEM images of Ag nanowire networks corresponding to different sheet resistance values: (a) 10, (b) 33, (c) 57, and (d) 103 Ω/sq.

Figure 3. As the Ag NW density increases, fewer voids remain in the films, leading to more uniform electrical field distribution realized using the Ag NW-based TCE. By tuning the density, a sheet resistance of ∼30 Ω/sq can be achieved, which is comparable to the performance of ITO on GaN for LED application. As shown in Figure 3, the holes in the Ag NW films are in the range of 1−2 μm for 156 Ω/sq, whereas that in the Ag NW films are in the rage of 50−100 nm for 30 Ω/sq or vice versa. So, decrease in sheet resistance with increasing NW density can be attributed to the increase in conducting paths.

Although the Ag NW-based TCE itself has shown excellent performance in LEDs, it requires a high-quality contact with the p-GaN layer, i.e., ohmic contact. It is reported that the Ag NW mesh electrode with coating of surfactant molecules of

DOI: 10.1021/am509116s
ACS Appl. Mater. Interfaces 2015, 7, 7945−7950

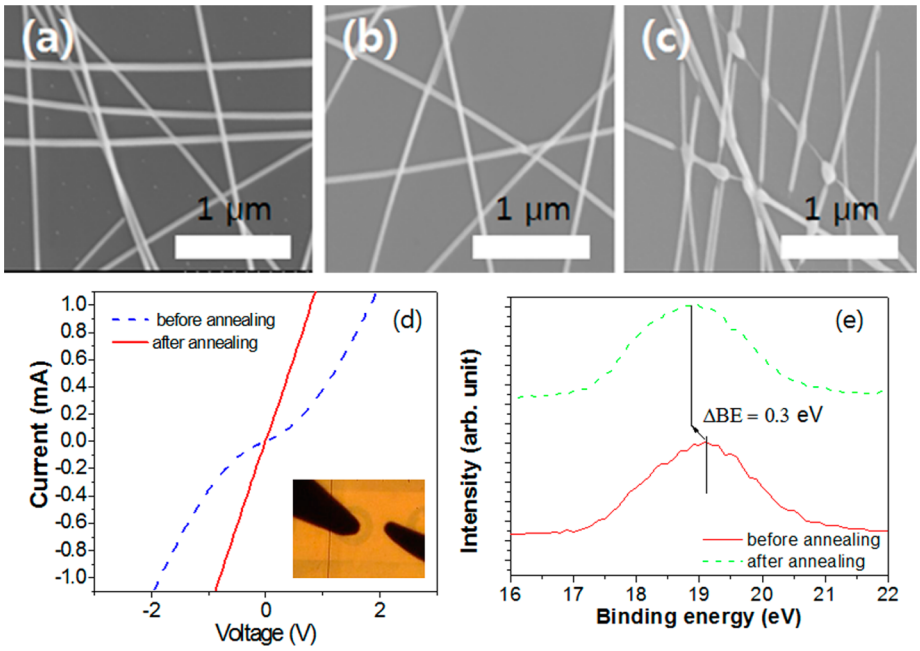

Figure 4. SEM images of Ag nanowire networks corresponding to different annealing temperatures of (a) 100, (b) 200, and (c) 300 °C. (d) Current−voltage characteristics of Ag nanowire network after and before annealing (gap = 10 μm), and (e) the Ga 3d core level for the Ag NW/GaN interface regions before and after annealing.

polyvinylpyrrolidone (PVP) can result in high initial resistance to prevent the formation of Ohmic contact.[8] To create an Ohmic contact between the Ag NW-based TCE and p-GaN, it is important to decrease the contact resistance by promoting out-diffusion of Ga atoms at the interface.[27] To analyze the current−voltage (I−V) characteristics, a lithography process was used to define circular structures by the circular transmission line model (CTLM) method. The inner circular contact had a diameter of 100 μm, and gaps between inner and outer contacts were 20 μm. In general, to form the Ohmic contact of Ag to p-GaN, high temperature above 300 °C was used.[20−22] However, we found that the Ag NWs are agglomerated above 300 °C as shown in Figure 4a−c, resulting in an increase in sheet resistance. With optimization of annealing condition, it was found that after annealing at 150 °C for 10 min, the measured I−V curves of Ag NW-based TCE exhibit fairly good Ohmic behavior while that of Ag NW-based TCE before annealing shows Schottky behavior, as shown in Figure 4d. The specific contact resistance is 2.5×10^{-3} Ω cm^2. The specific contact resistance of Ag NW is still lower than the reported value for the Ag film.[20−22] This can be attributed to a low annealing temperature and PVP-coated Ag NW. However, this value is comparable to that of ITO/p-GaN (1×10^{-4} to 1×10^{-3} Ω cm^2).[27,28] To clearly understand improve Ohmic behavior after annealing, we added the XPS measurement. To characterize the chemical bonding state of Ga, we made an XPS examination of the Ag NW contact on p-GaN before and after annealing. Before starting analysis, the Ag NW was sputtered using Ar+ ions to expose the interface region between the contact layer and GaN. Figure 4e shows the Ga 3d core level for the conact/p-GaN interface regions before and after annealing. It is evident that the Ga 3d core level for the annealed sample shifts toward the lower energy side by 0.3 eV compared to the as-deposit sample. This indicates that annealing causes a shift of the surface Fermi level toward the valence bandedge and hence, the reduction of band bending in p-GaN, resulting in improvement of Ohmic behavior.

To clearly understand the improvement in electrical properties as a result of annealing, we measured the cross-sectional TEM images. As expected, images a and b in Figure 5 show the 3 nm thick insulating coating of PVP on the side of Ag NW, resulting from the strong interaction between PVP and Ag.[29] Although PVP was strongly adsorbed on side surfaces of Ag NWs, it is readily decomposed by the annealing process. Therefore, it is expected that Ag and Ga atoms can easily

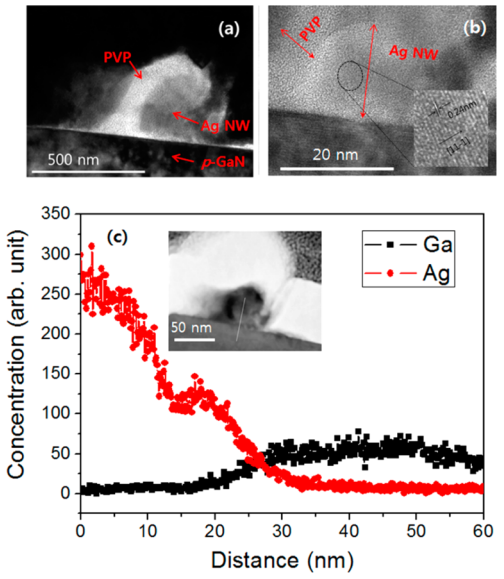

Figure 5. (a) Cross-sectional TEM image at the interface between p-GaN and Ag nanowires (NW). (b) Magnified cross-sectional TEM image at the interface between p-GaN and Ag NW. (c) Atomic concentration of Ga and Ag as a function of distance, as determined by energy-dispersive spectroscopy analysis.

DOI: 10.1021/am509116s
ACS Appl. Mater. Interfaces 2015, 7, 7945−7950

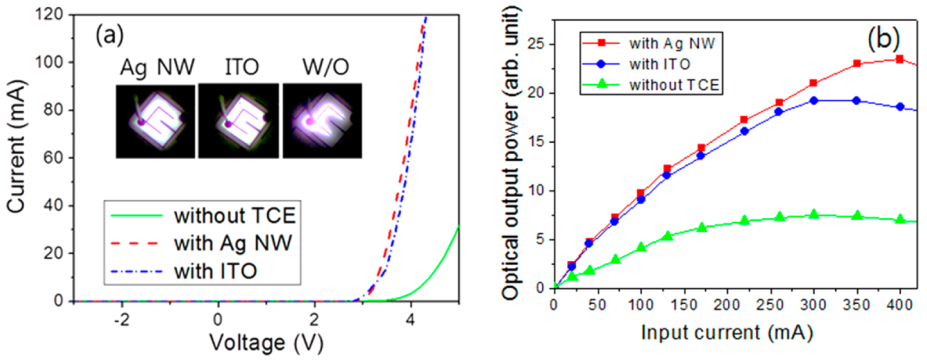

Figure 6. (a) Current−voltage characteristics and (b) optical output power of UV LED without transparent conductive electrode (TCE) and with Ag NW- and ITO-based TCE.

interdiffuse during the annealing process at the interface between p-GaN and the Ag NW mesh. Figure 5b also shows the single-crystalline nature of the Ag NW. The lattice spacing is measured to be 0.24 nm, agreeing well with that of [11−1] plane of face centered cubic (fcc) Ag. To understand the decrease in the contract resistance by interdiffusion process, we performed the energy-dispersive spectroscopy (EDS) at the interface between the Ag NW mesh and p-GaN after thermal annealing. EDS−scanning transmission electron microscopy (STEM) was utilized to characterize the distribution of Ag and Ga ath the interface between p-GaN and Ag NW TCE. Figure 5c shows the considerable amount of intermixing at the interface. In addition, some amount of Ga out-diffused into the metal layer. These results indicate a possible reaction between Ga and Ag, resulting in the formation of interfacial gallide. Therefore, the contact resistance decreased with increasing hole concentration because of the increasing number of Ga vacancies that act as acceptors.[30]

Figure 6a displays the *I*−*V* curves of InGaN/GaN LEDs with and without the Ag NW-based TCE, and with the ITO-based TCE. When the injection current was 20 mA, the forward voltages of the LEDs with and without the Ag NW-based TCE and with the ITO-based TCE were measured to be 3.47, 4.6, and 3.55 V, respectively. These results indicate that the electrical properties of the LED did not deteriorate when the Ag NW-based TCE was used, because the electrical characteristics of Ag NWs are comparable to those of ITO. The inset of Figure 6a shows the electroluminescent emission image of LEDs with the Ag NW- and ITO-based TCEs, and without a TCE. This figure clearly indicates that the current injection and current spreading in the case of the UV LED with the Ag NW- and ITO-based TCEs were better than those in the case of the LED without the TCE. Figure 6b displays the light output power of the InGaN/GaN LEDs with and without the Ag NW-based TCE and with the ITO-based TCE. The light output intensity (at an injection current of 100 mA) of the LED with the Ag NW-based TCE was three times higher than the output intensity of the LED without a TCE. Light output power enhancement of the GaN-based UV LEDs with Ag NW compared to that of with ITO is 7.4 and 20.1% at an input current of 100 mA and 350 mA. The optical output power of the LED with the Ag NW-based TCE was slight higher and degraded more slowly than that of the LED with the ITO-based TCE and p-GaN. This can be attributed to improvement of heat spreading by high thermal conductivity of Ag NW-based TCE, compared to that of ITO.[31]

The results of this study demonstrate that the Ag NW-based TCE meets the most important criteria related to conductivity and transparency, necessary to replace ITO in LEDs. In addition, the electrical and optical properties of a UV LED with the Ag NW-based TCE were better than those of a UV LED with an ITO-based TCE. A significant improvement in the electrical and optical properties of the LED is expected after optimization of conductivity and transparency through the control of density, size, and method of deposition of Ag NWs, improvement of Ohmic behavior and optimization of plasmonic effect for light extraction in AlGaN-based UV LED, suggesting that the use of a Ag NW-based TCE is a very promising way to develop high-efficiency UV LEDs as a solid-state light source.

CONCLUSION

In this work, we demonstrate the UV LED with a Ag NW-based TCE deposited by a simple spin-coating method. After optimization of the deposition conditions, the Ag NW-based TCE shows a sheet resistance of 30−40 Ω/sq and an optical transmittance of >85%, which is comparable to the characteristics of ITO-based TCEs. The UV LED with the Ag NW-based TCE has slightly better electrical and optical properties than ITO-based TCEs. We anticipate the application of the Ag NW-based TCE to a wide variety of devices, including UV LEDs, with lower fabrication costs and improved performances.

AUTHOR INFORMATION

Corresponding Author

*E-mail: mkkwon@chosun.ac.kr.

Author Contributions

The manuscript was written through contributions of all authors. All authors have given approval to the final version of the manuscript.

Notes

The authors declare no competing financial interest.

ACKNOWLEDGMENTS

This study was supported by the Basic Science Research Program through the National Research Foundation of Korea (NRF) funded by the Ministry of Education, Science and Technology (Project 2010-0024087) and Leading Industry Development for Honam region (Project R0001963).

DOI: 10.1021/am509116s
ACS Appl. Mater. Interfaces 2015, 7, 7945−7950

REFERENCES

(1) Schubert, E. F.; Kim, J. K. Solid-State Light Sources Getting Smart. *Science* **2005**, *308*, 1274−1278.

(2) Khan, A.; Balakrishnan, K.; Katona, T. Ultraviolet Light-Emitting Diodes Based on Group Three Nitrides. *Nat. Photonics* **2008**, *2*, 77−84.

(3) Pan, C.; Lee, C. M.; Liu, J. W.; Chen, G. T.; Chyi, J. I. Luminescence Efficiency of InGaN Multiple-Quantum-Well Ultraviolet Light-Emitting Diodes. *Appl. Phys. Lett.* **2009**, *84*, 5249−5251.

(4) Kuo, C. H.; Chang, S. J.; Su, Y. K.; Chuang, R. W.; Chang, C. S.; Wu, L. W.; Lai, W. C.; Chen, J. F.; Sheu, J. K.; Lo, H. M.; Tasi, J. M. Nitride-based Near-Ultraviolet LEDs with an ITO Transparent Contact. *Mater. Sci. Eng., B* **2004**, *106*, 69−72.

(5) Kim, H.; Cilmore, C. M.; Pique, A.; Horwitz, J. S.; Mattoussi, H.; Murata, H.; Kafafi, Z. H.; Chrisey, D. B. Electrical, Optical, and Structural Properties of Indium-Tin-Oxide Thin Films for Organic Light-Emitting Devices. *J. Appl. Phys.* **1999**, *86*, 6451−6461.

(6) Seo, T. H.; Lee, K. J.; Park, A. H.; Hong, C. H.; Shu, E. K.; Chae, S. J.; Lee, Y. H.; Cuong, T. V.; Pham, V. H.; Chung, J. S.; Kim, E. J.; Jeon, S. R. Enhanced Light Output Power of Near UV Light Emitting Diodes with Graphene/Indium Tin Oxide Nanodot Nodes for Transparent and Current Spreading Electrode. *Opt. Express* **2011**, *19*, 23111−231117.

(7) Guo, H.; Lin, N.; Chen, Y.; Wang, Z.; Xie, Q.; Zheng, T.; Gao, N.; Li, S.; Kang, J.; Cai, D.; Peng, D. Copper Nanowires as Fully Transparent Conductive Electrodes. *Nat. Sci. Rep.* **2013**, *3*, 2323.

(8) Lee, J. Y.; Connor, S. T.; Cui, Y.; Peumans, P. Solution-Processed Metal Nanowire Mesh Transparent Electrodes. *Nano Lett.* **2008**, *8*, 689−692.

(9) Scardaci, V.; Coull, R.; Lyons, P. E.; Rickard, D.; Coleman, J. N. Spray Deposition of Highly Transparent, Low-Resistance Networks of Silver Nanowires over Large Areas. *Small* **2011**, *7*, 2621−2628.

(10) Wu, H.; Kong, D.; Ruan, Z.; Hsu, P. C.; Wang, S.; Yu, Z.; Carney, T. J.; Hu, L.; Fan, S.; Cui, Y. A Transparent Electrode Based on a Metal Nanotrough Network, Nat. *Nanotechnology* **2013**, *8*, 421−425.

(11) Kim, K. H.; An, H.; Kim, H.; Kim, T. G. Transparent Conductive Oxide Films Mixed with Gallium Oxide Nanoparticle/Single-Walled Carbon Nanotube Layer for Deep Ultraviolet Light-Emitting Diodes. *Nanoscale Res. Lett.* **2013**, *8*, 507.

(12) Gao, J.; Mu, X.; Ki, X.; Wang, W.; Meng, Y.; Xu, X.; Chen, L.; Cui, L.; Wu, X.; Geng, H. Modification of Carbon Nanotube Transparent Conducting Films for Electrodes in Organic Light-Emitting Diodes. *Nanotechnology* **2013**, *24*, 435201.

(13) Wu, J. B.; Agrawal, M.; Becerril, H. A.; Bao, Z. N.; Liu, Z. F.; Chen, Y. S.; Peumans, P. Organic Light-Emitting Diodes on Solution-Processed Graphene Transparent Electrodes. *ACS Nano* **2010**, *4*, 43−48.

(14) Yu, Z.; Zhang, Q.; Li, L.; Chen, Q.; Niu, X.; Liu, J.; Pei, Q. Highly Flexible Silver Nanowire Electrodes for Shape-Memory Polymer Light-Emitting Diodes. *Adv. Mater.* **2011**, *23*, 664−668.

(15) Zhu, R.; Chung, C.; Cha, K. C.; Yang, W.; Zheng, Y. B.; Zhou, H.; Song, T.; Chen, C.; Weiss, P. S.; Li, G.; Yang, Y. Fused Silver Nanowires with Metal Oxide Nanoparticles and Organic Polymers for Highly Transparent Conductors. *ACS Nano* **2011**, *5*, 9877−9882.

(16) Hu, L. B.; Kim, H. S.; Lee, J. Y.; Peuman, P.; Cui, Y. Scalable Coating and Properties of Transparent, Flexible, Silver Nanowire Electrodes. *ACS Nano* **2010**, *4*, 2955−2963.

(17) OK, K.; Kim, J.; Park, S.; Kim, Y.; Lee, C.; Hong, S.; Kwak, M.; Kim, N.; Han, C. J.; Kim, J. Ultra-thin and Smooth Transparent Electrode for Flexible and Leakage-free Organic Light-Emitting Diodes. *Nat. Sci. Rep.* **2015**, *5*, 9464.

(18) Seo, T. H; Kim, B. Y.; Shin, G.; Lee, C.; Kim, M. J.; Kim, H.; Suh, E. Graphene-Silver Nanowire Hybrid Structure as a Transparent and Current Spreading Electrode in Ultraviolet Light Emitting Diodes. *Appl. Phys. Lett.* **2013**, *103*, 051105.

(19) Seo, T. H.; Park, A. H.; Park, S.; Chandramohan, S.; Lee, G. H.; Kim, M. J.; Hong, C.; Suh, E. Improving the graphene electrode performance in ultra-violet light-emitting diode using silver nanowire networks. *Opt. Mater. Express* **2015**, *1*, 314−322.

(20) Serway, R. A. *Principles of Physics*, 2nd ed.; Saunders College Publishing: Fort Worth, TX, 1998.

(21) Song, J.; Kwak, J. S.; Park, Y.; Seong, T. Y. Ohmic and Degradation Mechanisms of Ag Contacts on p -type GaN. *Appl. Phys. Lett.* **2005**, *86*, 062104.

(22) Kim, J. Y.; Na, S. I.; Ha, G. Y.; Kwon, M. K.; Park, I. K.; Lim, J. H.; Park, S. J.; Kim, M. H.; Choi, D.; Min, K. Thermally Stable and Highly Reflective AgAl Alloy for Enhancing Light Extraction Efficiency in GaN Light-Emitting Diodes. *Appl. Phys. Lett.* **2006**, *88*, 043507.

(23) Tao, A.; Kim, F.; Hess, C.; Goldberger, J.; He, R. R.; Sun, Y. G.; Xia, Y. N.; Yang, P. D. Langmuir−Blodgett Silver Nanowire Monolayers for Molecular Sensing Using Surface-Enhanced Raman Spectroscopy. *Nano Lett.* **2003**, *3*, 1229−1233.

(24) Allione, M.; Temnov, V. V.; Fedutik, Y.; Woggon, U.; Artemyev, M. V. Surface Plasmon Mediated Interference Phenomena in Low-Q Silver Nanowire Cavities. *Nano Lett.* **2008**, *8*, 31−35.

(25) Kwon, M. K.; Kim, J. Y.; Kim, B. H.; Park, I. K.; Cho, C. Y.; Byeon, C. C.; Park, S. J. Surface-Plasmon-Enhanced Light-Emitting Diodes. *Adv. Mater.* **2008**, *20*, 1253−1257.

(26) Xie, S.; Ouyang, Z.; Stokes, N.; Jia, B.; Gu, M. Enhancing the Optical Transmittance by using Circular Silver Nanowire Networks. *J. Appl. Phys.* **2014**, *115*, 193102.

(27) Lui, Y.; Huang, C.; Chen, T.; Hsu, C.; Liou, J.; Tsai, T.; Liu, W. Implementation of an Indium-Tin-Oxide (ITO) Direct-Ohmic Contact Structure on a GaN-based Light Emitting Diode. *Opt. Express* **2011**, *19*, 14662−14670.

(28) Zhang, Y.; Li, X.; Wang, L.; Yi, X.; Wu, D.; Zhu, H.; Wang, G. Enhanced Light Emission of GaN-Based Diodes with a NiOx/Graphene Hybrid Electrode. *Nanoscale* **2012**, *4*, 5852−5855.

(29) Sun, Y.; Yin, Y.; Mayers, B. T.; Herricks, T.; Xia, Y. Uniform Silver Nanowires Synthesis by Reducing $AgNO_3$ with Ethylene Glycol in the Presence of Seeds and Poly(Vinyl Pyrrolidone). Chem. *Meter.* **2002**, *14*, 4736−4745.

(30) Song, J. O.; Leem, D. S.; Seong, T. Y. Formation of low resistance and transparent ohmic contacts to p-type GaN using Ni-Mg solid solution. *Appl. Phys. Lett.* **2003**, *83*, 3513−3515.

(31) Han, N.; Tran, T. V.; Han, M.; Ryu, B. D.; Chandramohan, S.; Park, J. B.; Kang, J. H.; Park, Y.; Ko, K. B.; Kim, H. Y.; Kim, H. K.; Ryu, J. H.; Katharria, Y. S.; Choi, C.; Hong, C. Improved Heat Dissipation in Gallium Nitride Light-Emitting Diodes with Embedded Graphene Oxide Pattern. *Nature Commun.* **2013**, *4*, 1452.

DOI: 10.1021/am509116s
ACS Appl. Mater. Interfaces 2015, 7, 7945−7950